



HAL
open science

alpha-Skeletal muscle actin nemaline myopathy mutants cause cell death in cultured muscle cells.

Drieke Vandamme, Ellen Lambert, Davy Waterschoot, Christian Cognard, Joël Vandekerckhove, Christophe Ampe, Bruno Constantin, Heidi Rommelaere

► To cite this version:

Drieke Vandamme, Ellen Lambert, Davy Waterschoot, Christian Cognard, Joël Vandekerckhove, et al.. alpha-Skeletal muscle actin nemaline myopathy mutants cause cell death in cultured muscle cells.. *Biochimica et Biophysica Acta - Molecular Cell Research*, 2009, 1793 (7), pp.1259-1271. 10.1016/j.bbamcr.2009.04.004 . hal-02880249

HAL Id: hal-02880249

<https://hal.science/hal-02880249>

Submitted on 17 Nov 2022

HAL is a multi-disciplinary open access archive for the deposit and dissemination of scientific research documents, whether they are published or not. The documents may come from teaching and research institutions in France or abroad, or from public or private research centers.

L'archive ouverte pluridisciplinaire **HAL**, est destinée au dépôt et à la diffusion de documents scientifiques de niveau recherche, publiés ou non, émanant des établissements d'enseignement et de recherche français ou étrangers, des laboratoires publics ou privés.



Distributed under a Creative Commons Attribution - NonCommercial - NoDerivatives 4.0 International License



Contents lists available at ScienceDirect

Biochimica et Biophysica Acta

journal homepage: www.elsevier.com/locate/bbamcr

α -Skeletal muscle actin nemaline myopathy mutants cause cell death in cultured muscle cells

Drieke Vandamme^{a,b}, Ellen Lambert^{a,b,1}, Davy Waterschoot^{a,b}, Christian Cognard^c, Joël Vandekerckhove^{a,b}, Christophe Ampe^{a,b,*}, Bruno Constantin^c, Heidi Rommelaere^{a,b,2}

^a Department of Biochemistry, Faculty of Medicine and Health Sciences, Ghent University, A. Baertsoenkaai 3, B-9000, Gent, Belgium

^b Department of Medical Protein Research, VIB, A. Baertsoenkaai 3, Gent, Belgium

^c Institut de Physiologie et Biologie Cellulaire, UMR CNRS/Université de Poitiers 6187, Pôle Biologie Santé, 86022 Poitiers cedex, France

ARTICLE INFO

Article history:

Received 23 December 2008

Received in revised form 24 March 2009

Accepted 14 April 2009

Available online xxx

Keywords:

Actin
Nemaline myopathy
Myoblast
Myotube
Cell death

ABSTRACT

Nemaline myopathy is a neuromuscular disorder, characterized by muscle weakness and hypotonia and is, in 20% of the cases, caused by mutations in the gene encoding α -skeletal muscle actin, *ACTA1*. It is a heterogeneous disease with various clinical phenotypes and severities. In patients the ultrastructure of muscle cells is often disturbed by nemaline rods and it is thought this is the cause for muscle weakness. To search for possible defects during muscle cell differentiation we expressed α -actin mutants in myoblasts and allowed these cells to differentiate into myotubes. Surprisingly, we observed two striking new phenotypes in differentiating myoblasts: rounding up of cells and bleb formation, two features reminiscent of apoptosis. Indeed expression of these mutants induced cell death with apoptotic features in muscle cell culture, using AIF and endonuclease G, in a caspase-independent but calpain-dependent pathway. This is the first report on a common cellular defect induced by NM causing actin mutants, independent of their biochemical phenotypes or rod and aggregate formation capacity. These data suggest that lack of type II fibers or atrophy observed in nemaline myopathy patients may be also due to an increased number of dying muscle cells.

© 2009 Elsevier B.V. All rights reserved.

1. Introduction

Nemaline myopathy (NM) is a neuromuscular disorder, characterized by muscle weakness and hypotonia. It is a heterogeneous disease in which cases are classified according to the onset of the illness and clinical presentation of patients [1,2] ranging from lethality shortly after birth to having a fairly normal life. NM is a disease of the skeletal muscle sarcomere and is caused by mutations in some components of the thin filament [3] and in particular in α -skeletal muscle actin (*ACTA1*, further referred to as α -actin) [4–6]. At the cellular level a typical phenotype is the presence of rod shaped structures (nemaline rods) that disturb muscle ultrastructure and that contain actin. They are either present in the sarcoplasm or in the nuclei of affected muscle fibers. On this bases NM has been further divided into subclasses [6], typical nemaline myopathy (NEM) and intranuclear rod myopathy (IRM) respectively. A third class, actin myopathy (AM), is characterized by an excess of thin filamentous inclusions disturbing the normal myofibrillar filament lattice. This division in three classes is, however, not strict since a number of patients show more than one histological

phenotype in their muscle biopsies, such as the combination of intranuclear rods with excess of thin filament or with cytoplasmic rods. The rods contain actin and material from Z-lines, mainly α -actinin 2 [7]. However, their composition and size vary depending on their subcellular location [8]. Curiously, the proportion of muscle fibers with rods does not correlate with the degree of muscle weakness [1].

To date, more than 100 α -actin mutations leading to NM have been identified [9,10]. It is not surprising that mutations in this highly conserved protein cause muscle diseases, given its importance in striated muscle formation and function, and its complex activities. Actin requires a special folding pathway, involving the chaperones prefoldin and the cytoplasmic chaperonin CCT, for functional maturation [11–13]. It has an absolute requirement for ATP (or ADP) to remain stable [14]. It self-associates resulting in the formation of actin filaments that are part of the cytoskeleton and that can interact with many actin binding proteins (ABPs), e.g. α -actinin, troponin and myosin in muscle, thereby contributing to contractile force generation. As a result, a disease causing mutation in actin may affect one or more of these properties, and some of these defects can be unraveled by biochemical tests and/or by ectopic expression in fibroblasts or myoblasts and early myotubes as shown in previous studies by us and by others [15–17]. However, there is little correlation between biochemical behaviour and cell biological or even clinical observations.

* Corresponding author. Department of Biochemistry, Ghent University, A. Baertsoenkaai 3, B-9000 Gent, Belgium. Tel.: +32 9 264 93 36; fax: +32 9 264 94 88.

E-mail address: Christophe.Ampe@ugent.be (C. Ampe).

¹ Present address: Department of Plant Production, Faculty of Bioscience Engineering, UGent, Coupure links 653, Gent, Belgium.

² Present address: Ablynx N.V., Technologiepark 4, 9052 Zwijnaarde, Belgium.

In the present study we characterized a new set of NM causing α -skeletal actin mutants biochemically and by expression in fibroblasts, myoblasts and myotubes. Upon expression of two mutants displaying folding defects (L140P and G146D) in differentiating myoblasts, we observed two striking new phenotypes: bleb formation at the cell membrane and rounding up of cells, two features reminiscent of apoptosis. These features were also observed upon inspection of differentiating myotubes expressing these or other NM causing actin mutants. Our results indicate that these mutants induce cell death in muscle cell culture in a caspase-independent, calpain involved AIF and endonuclease G pathway. The observed cell death occurs regardless of the biochemical or cellular phenotypes of the α -actin mutants. Thus for the first time we found a common muscle cell specific defect induced by NM causing actin mutants and these data suggest that atrophy, with a lack of type II fibers, commonly observed in NM patients may be in part due to increased cell death.

2. Materials and methods

2.1. Construction of the α -actin nemaline myopathy mutants

Mutations were made with the QuikChange site directed mutagenesis kit (Stratagene) according to the manufacturer's instructions, using the human *ACTA1* cDNA sequence in pcDNA3.1 (Invitrogen) as a template and appropriate primers. N-terminal myc-tagged wild type actin and mutants were made by PCR using the actin (mutants) in the pcDNA3.1 vector as template, a 5' primer containing the myc-sequence preceded by a HindIII site and a 3' primer containing an XbaI site. These fragments were ligated into HindIII–XbaI digested pcDNA3.1. pIRES-GFP Wt and mutant constructs were made by PCR with a 5' primer containing an XhoI site and a 3' primer containing a BamHI site and ligated in the XhoI–BamHI digested pIRES-EFGP2 vector. Constructs were sequenced to verify the complete *ACTA1* coding sequence and correct introduction of the desired mutation. Expression of actin mutants using *in vitro* translation assays, band shift assays with actin binding proteins, and copolymerization assays were performed as described in [16,18].

2.2. Cell culture and transfection

Sol8 myogenic cells [19] were seeded in 12 well plates containing gelatin-coated glass or thermanox coverslips (Nunc). Myoblasts were grown in Dulbecco's modified Eagle medium (DMEM)/HamF-12 medium (Invitrogen) (50:50) supplemented with 10% fetal calf serum (Invitrogen), 1% L-glutamine, and 1% antibiotics (penicillin-G, 100 IU/ml and streptomycin, 100 μ g/ml, Invitrogen). After 24 h the cells were transfected with the pcDNA3.1 vectors encoding N-terminally myc-tagged α -skeletal muscle actin (wild type or mutant) using jetPEI (Qbiogene) or the Effectene transfection reagent (Qiagen) according to the manufacturer's protocols. To study transfected myoblasts, coverslips were mounted for immunofluorescence after 48 h of transfection. To promote fusion (F) of myoblasts into myotubes, the growth medium was replaced by a differentiation medium (DMEM supplemented with 2% heat-inactivated horse serum (Invitrogen), 10 μ g/ml insulin (Sigma), 1% L-glutamine and 1% antibiotics, following 2–3 days of proliferation (37 °C, 5% CO₂, water-saturated air) to around 80% of confluence). Myotubes were immunostained on day F+4. Sometimes myotubes were kept in culture till 11 days after fusion; they were seeded on thermanox coverslips and the proliferation medium contained only 0.5% horse serum and no insulin. Sol8 cells were transfected using the Amaxa cell line nucleofector kit V, according to the manufacturer's instructions. We used nucleofection for the transfection experiments since this resulted in a much higher transfection yield, which is required for counting dying cells, in order to have statistically reliable data and interpretations.

For primary cultures, satellite cells were isolated from hind limb muscles of newborn rats. Muscles were minced and washed in a calcium- and magnesium-free medium (116 mM NaCl; 5 mM KCl; 2.6 mM NaHCO₃; 8 mM NaH₂PO₄; pH 7.5; 4 °C) and then transferred in the same medium containing trypsin (250 U/mg, Seromed) for two rounds of dissociation (10 min and 20 min, respectively; 37 °C) with continuous stirring. The supernatants were centrifuged (15 min at 4 °C, 700 \times g) and the pellets were resuspended in a 78% HAM F-12 medium, supplemented with 10% fetal calf serum, 10% heat-inactive horse serum, 1% L-glutamine and 1% antibiotics. The cell suspension was then filtered on a nylon netting (pore size 21 μ m) in culture flasks and preplated in 100 mm plastic petri-dishes for 40 min (37 °C, 5% CO₂, water-saturated air) to remove most of the adhering non-muscle cells. Then cells were seeded on laminin-coated glass coverslips in 12 well plates. After 48 h, cells were transfected with the pcDNA3.1 vectors encoding N-terminally myc-tagged α -skeletal muscle actin (wild type or mutant) using jetPEI (Qbiogene). After 1 day (F) the growth medium was exchanged for a fusion medium: DMEM supplemented with 5% heat-inactivated horse serum. Myotubes were immunostained on day F+4.

2.3. Calculation of fusion index and % of rounded cells

For the calculation of fusion indexes we determined the amount of nuclei (DAPI staining) in myotubes (phase contrast) and divided this by the total amount of nuclei. This was done for two independent experiments and the mean was calculated.

We determined for each mutant the percentage of round or spindle shaped blebbing cells of the total transfected (myc or EGFP-positive) population on a coverslip (~900 to 3000 cells) after 4 days of differentiation. We calculated the mean of two independent experiments per mutant.

2.4. Immunological staining

The cultured cells were fixed in TBS/4% paraformaldehyde and permeabilized with TBS/0.5% Triton X-100. Samples were then incubated for 1 h with primary antibodies (polyclonal anti-myc antibody (Abcam) to visualise the mutant actins and a monoclonal antibody against troponin T (Sigma), or α -actinin (Sigma) to visualise myofilaments) in TBS (20 mM Tris base, 154 mM NaCl, 2 mM EGTA, 2 mM MgCl₂, pH 7.5)/1% BSA (Sigma). After washing in TBS, the cells were incubated for 30 min in TBS/1% BSA with FITC-conjugated goat anti-mouse and TRITC-conjugated anti-rabbit secondary antibodies or TRITC-phalloidin (Jackson ImmunoResearch). Samples were mounted using Vectashield mounting medium (Vector). Nuclei were stained with the TO-PRO-3 dye (Molecular Probes) or with DAPI (Molecular probes).

2.5. Detection of apoptosis

Transfected cells were stained for the myc-tagged actin and co-stained either with a mouse anti-cytochrome c antibody using the select FX alexa fluor 488 cytochrome c apoptosis detection kit (Invitrogen), a rabbit anti-cleaved caspase-3, anti-caspase-3, anti-cleaved caspase-9, anti-caspase-12 or anti-cleaved PARP antibody (Cell Signalling Technology), a mouse anti-AIF antibody (Santa Cruz Biotechnology) or a rabbit anti-endo G antibody (Abcam). As a positive control for apoptosis, cells were incubated for 4 h with 10 μ M camptothecin (Sigma) at 37 °C before staining (data not shown) or 2 μ M staurosporin for 24 h. For analysis of fluorescence intensity of cleaved caspase 3, 5 regions of interest were selected and the mean fluorescence intensity of every region was measured. The mean of these 5 averages was calculated.

For Western blots cells were lysed in PBS with 1% Triton X-100, 1 μ g/ml leupeptin, 1 μ g/ml aprotinin, 1 μ g/ml antipain, 1.6 μ g/ml

benzamidin, and 1 $\mu\text{g/ml}$ pepstatin. Standard procedures for Western blotting were used with rabbit anti-caspase 2 (Abcam) or a rabbit anti-cleaved caspase 3, anti-cleaved caspase-9, anti-caspase-12 or anti-cleaved PARP antibody (Cell Signalling Technology).

To probe for caspase and calpain activity we added to the differentiation medium 5 or 10 μM of the pancaspase inhibitor ZVAD-FMK (promega) or 50 μM PD150606 calpain inhibitor (Calbiochem), respectively during 4 days of differentiation.

2.6. Cytofluorescence analysis

Immunolabeled samples were examined using an Olympus IX71 epifluorescence microscope and images were acquired using a cooled Spot Camera (Diagnostic Instruments) and Analysis software (Soft Imaging Systems). Images were also acquired using a Zeiss Axioplan 200 M epifluorescence microscope, equipped with an Apotome slider, a cooled CCD Axiocam Camera and Axiovision 4.4 software. Confocal laser-scanning microscopy (CLSM) was performed using a Bio-Rad MRC 1024 ES (Bio-Rad, Hemel Hempstead, UK) equipped with an argon–krypton gas laser. The TRITC fluorochrome was excited with the 568-nm yellow line and the emission was collected via a photomultiplier through a 585 long pass filter, the FITC fluorochrome with the 488 nm line and collected through the 522 filter. Nuclei staining was obtained with the TO-PRO-3 probe and acquired with excitation at 647 nm and collected through the 680 nm filter. Additionally, an Olympus confocal system equipped with an argon–krypton gas laser was used. The excitation wavelength of 488 nm and 543 nm were respectively used for acquisition of images in green channel (520 nm) and in red channel (600 nm). Data were acquired using an inverted microscope (Olympus IX70) with a $\times 60$ water immersion objective and processed with the LaserSharp software (version 3.0, Bio-Rad).

The mean fluorescence of myc staining of 38 WT and 40 A138P actin expressing Sol8 muscle cells (F+4) was measured with the Cell M software (Olympus).

3. Results

3.1. Biochemical characterization of seven new NM causing α -skeletal actin mutants

In a previous study [16], we biochemically characterized a set of actin mutants causing nemaline myopathy and discovered four different biochemical phenotypes: folding defective mutants, unstable mutants, mutants with reduced copolymerisation capacity and mutants without defects in these tests (for details and limitations of these assays see [16,18,20]). In the present study, we investigated seven new mutants using similar approaches. The locations of the mutations in the actin molecule are displayed in blue on the 3D-representation of the actin molecule (Fig. 1A) [21]. The mutations A138P, D154N, D179G and K336I are in or near the nucleotide-binding pocket, of which A138P and K336I are also in the hinge regions between actin subdomains 1 and 3, where also the mutations L140P and G146D are located. Mutation S348L is located in subdomain 1. In patient muscles, these mutants induce different abnormal structures such as intranuclear and cytoplasmic rods and/or an excess of thin filaments (Table 1).

Biochemical characterization revealed that actin mutants L140P and G146D display compromised folding (Fig. 1B). The majority of the synthesized molecules stick to the chaperones CCT and prefoldin. The few molecules that are released are however correctly folded, since they can bind to ABPs (Table 1). All other mutants fold properly since they migrate at a position similar to monomeric actin in gels containing ATP (Fig. 1B,b) and since they can bind with the ABPs tested (i.e. thymosin $\beta 4$, DNaseI and VDBP and adseverin, Table 1). Mutants α -act A138P, D154N, and D179G show an increase in CAP-binding on gels without ATP (respectively 28%, 35% and 9% compared

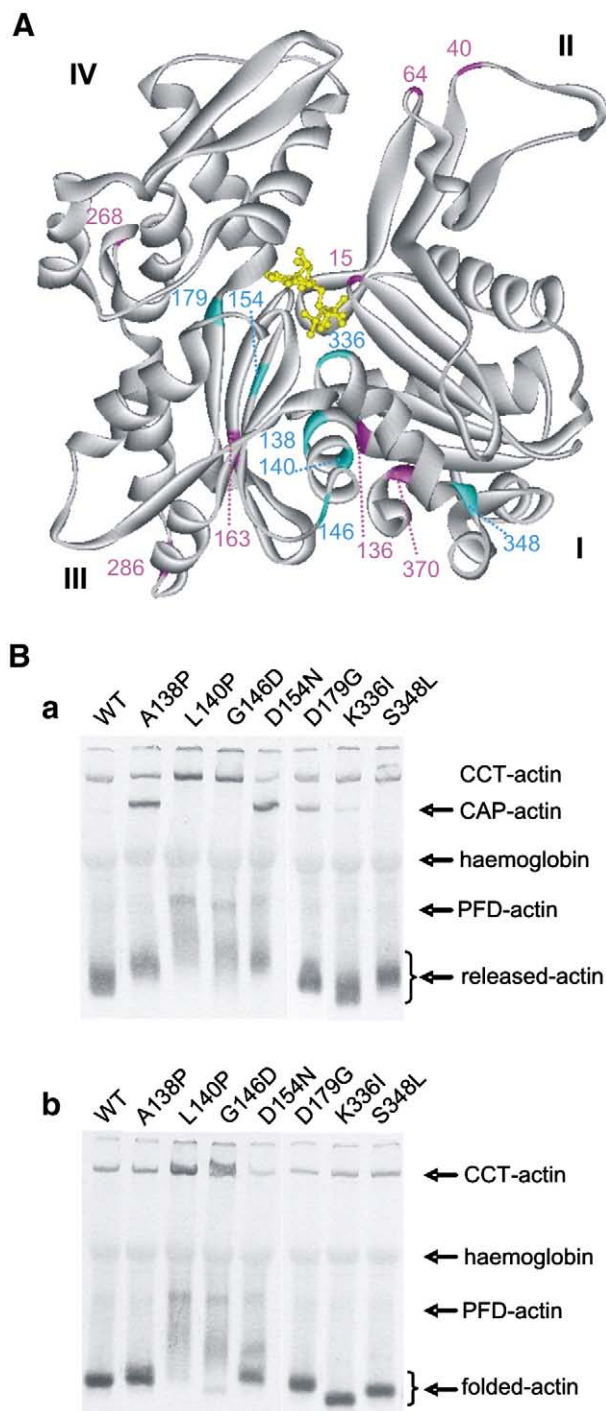


Fig. 1. (A) Location of the studied ACTA1 mutations on the 3D-representation of the actin molecule [21]. Mutants indicated in blue are biochemically characterized in this study; mutants in pink were biochemically characterized in Costa et al. [16]. I–IV indicate the actin subdomains. ATP is in yellow. The structure was taken from PDB code 1ATN and displayed by ViewerLite. (B) Native gel analysis and autoradiography of seven ^{35}S -labeled α -actin mutants causing NM and WT α -actin. Gels were run without (a) or with (b) ATP. Actins were produced in *in vitro* transcription translation reactions in reticulocyte lysate, which endogenously contains CAP [52] and the actin folding machinery, prefoldin (PFD) and CCT [11,13,18]. Mutants L140P and G146D remain bound to CCT and prefoldin under both conditions. The other mutants fold correctly, as evidenced by the presence of an abundance of folded actin. The different mobilities of the actins are due to the charge changes introduced by most of the mutations. On the gel without ATP, mutants α -act A138P, D154N and D179G show a pronounced increase in binding to CAP indicating they are less stable. (For interpretation of the references to colour in this figure legend, the reader is referred to the web version of this article.)

Table 1
Summary of the biochemical characterization of seven nemaline myopathy causing α -skeletal muscle actin mutants.

Mutant	Phenotype	Folding	CAP	ABP	Copol	In actin structure	Reference
WT		+	+	+	++		
A138P	IRM	+	+	+	++	Hinge region 1	[6]
L140P	Typical NEM	Few	–	+	+	Hinge region 1	[6]
G146D	AM	Few	–	+	+	Hinge region 1	[51]
D154N	AM, IRM	+	+	+	++	In ATP cleft	[50]
D179G	Severe NEM	+	+	+	++	In ATP cleft, stabilizing interaction with H73	[51]
K336I	IRM	+	+	+	++	In ATP cleft, ATP-binding	[6]
S348L	AM	+	–	+	++	In subdomain 1, at surface	[6,47]

The properties investigated here are folding, binding to cyclase associated protein (CAP), binding to the actin binding proteins (ABP) thymosin β 4, DNaseI and vitamin D binding protein (VDBP) and copolymerisation (copol) with rabbit α -skeletal muscle actin (copol). Also the position in the actin structure according to Kabsch et al. [21] is indicated, in addition to the phenotype of the patient as described in the reference, with AM = actin myopathy, excess of thin filaments; NEM = nemaline myopathy with sarcoplasmic nemaline bodies; IRM = intranuclear rod myopathy.

to 2% for WT) indicating they have impaired nucleotide binding [12,20], which is consistent with a mutation near the ATP-binding site. These mutants thus belong to the class of unstable mutants. The copolymerisation test allowed classifying the remaining mutants α -act K336I and S348L which show no copolymerisation defect *in vitro*.

3.2. WT myc-tagged α -skeletal muscle actin incorporates in myofilaments

To examine the ability of these actin mutants to incorporate into endogenous actin structures, we expressed N-terminal myc-tagged versions in Sol8 or primary myoblasts. We allowed them to differentiate and to fuse into myotubes and analysed the cellular phenotypes one (F+1), four (F+4) or five (F+5) days after induction of differentiation. Occasionally we also used NIH3T3 fibroblasts to illustrate a difference in behaviour of mutants in fibroblasts and myogenic cells.

Although undifferentiated myoblasts do not express endogenous α -actin ectopically, expressed myc-tagged WT α -actin incorporates in stress-fibers, which mainly consists of β -actin (Fig. 2A). This observation is consistent with the observation that precocious expression of α -skeletal muscle actin does not compromise the ability of myoblasts to form stress-fiber like structures [22].

During differentiation the myoblasts become spindle shaped (Fig. 2B, these myoblasts are further referred to as differentiating myoblasts) and fuse to long myotubes, initially with central nuclei (Fig. 2C). At this stage the main actin isoform is α -skeletal muscle actin. Staining for myc shows that ectopic WT α -actin incorporates in peripheric premyofibrils, but not in the internal phalloidin positive actin meshwork (Fig. 2B,C). Ectopic α -actin preferentially incorporates in the α -actin muscle specific cytoskeleton at more differentiated stages. This is also shown in cells that start to form striations, where myc-actin is incorporated in the nascent myofilaments decorated with α -actinin (Fig. 2D).

3.3. Folding compromised mutants do not incorporate into filamentous structures in cells and cause small bleb formation

Mutants α -act L140P and G146D do not incorporate in actin fibers in myoblasts, myotubes or fibroblasts consistent with their folding

defect observed *in vitro*. In fibroblasts they also do not form the rods (Fig. 3) that are typically observed for other NM causing actin mutants (see [16], and below). Rather these mutants are in phalloidin negative aggregates in fibroblasts (Fig. 3A) or diffusely localised in the cytoplasm of undifferentiated myogenic cells (Fig. 3D). Intriguingly in differentiating myoblasts they induce blebs and these are devoid of endogenous F-actin and troponin but do contain the mutant actin (Fig. 3B, E). In addition, in myotubes, both mutants do not incorporate in actin filaments, but reside in small speckles throughout the cytoplasm (Fig. 3C,F). Unlike WT transfected myotubes that have straight cell walls, L140P and G146D transfected myotubes occasionally display small blebs, in which mutant actin is locally enriched (arrows in Fig. 3F).

3.4. Actin mutants cause blebbing or rounding up of muscle cells during differentiation, independently of their biochemical phenotype

Given that bleb formation may be a new phenotype we investigated whether muscle cells expressing α -actin mutants with other biochemical defects (determined in this study or in [16], Fig. 1A) also display this phenotype during their differentiation. This indeed appears to be the case for some mutants with compromised ATP-binding: α -act G15R, A138P, D154N, V163L and D179G, for those with reduced copolymerisation capacity: α -act I64N, I136M and G268R and

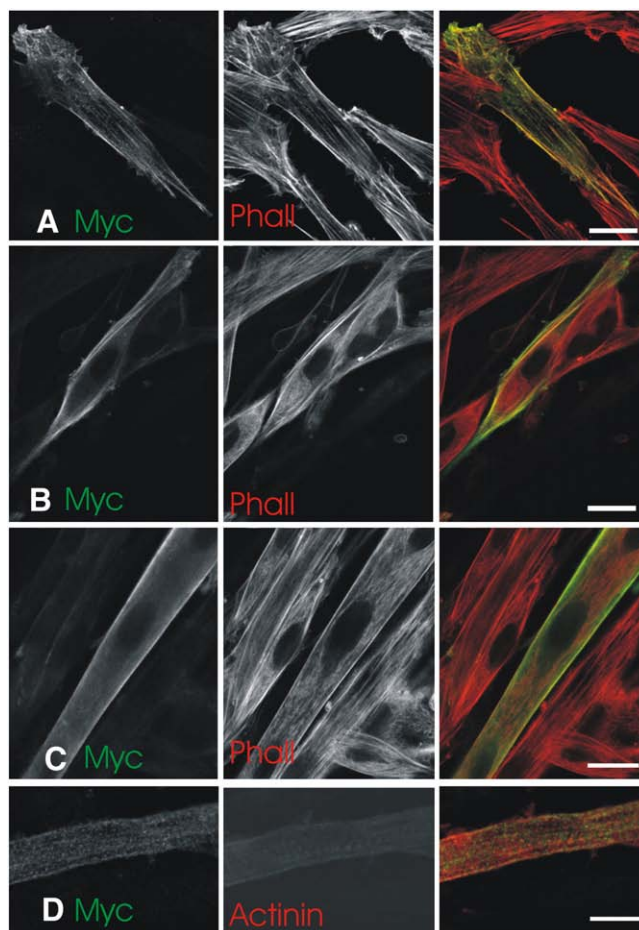
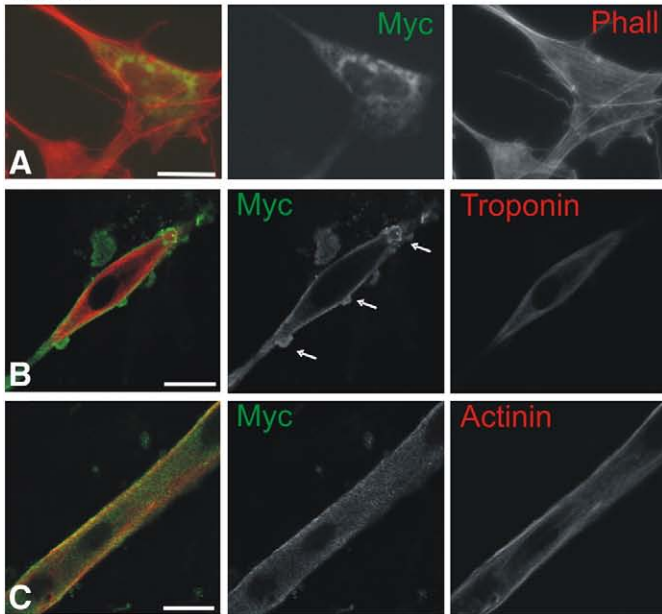


Fig. 2. N-terminally myc-tagged WT α -skeletal muscle actin incorporates normally in actin structures in myoblasts and myotubes. Myc-tagged WT α -actin colocalises with stress-fibers in undifferentiated myoblasts (A) and incorporates in peripheric premyofibrils in differentiating myoblasts (B) and early myotubes (F+4) (C); in more differentiated myotubes (F+5) myc-actin incorporates in the nascent sarcomeres. (D) Green is myc staining, red is phalloidin or actinin (D) staining. Images are confocal. Bars, 20 μ m. (For interpretation of the references to colour in this figure legend, the reader is referred to the web version of this article.)

L140P



G146D

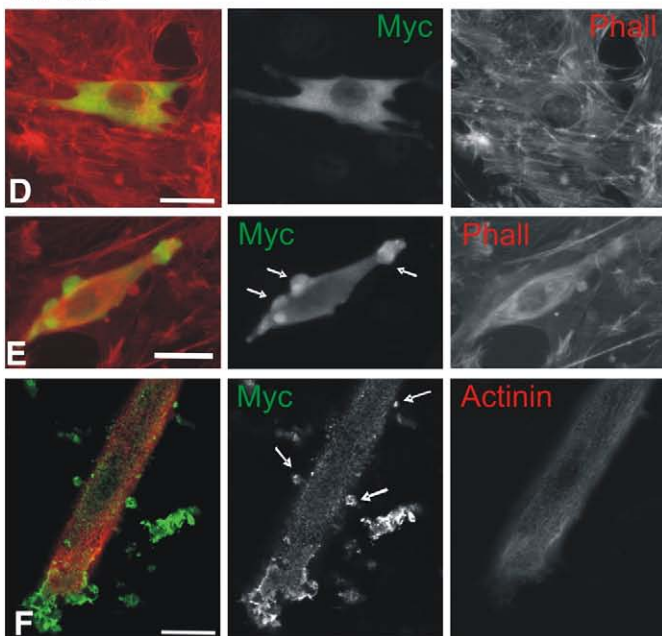


Fig. 3. α -actin mutants with folding defects do not incorporate in actin filaments and induce bleb formation in muscle cells. (A) NIH3T3 fibroblast, (B) differentiating Sol8 myoblast and (C) Sol 8 myotube (F+4) expressing myc- α -act L140P; (D) undifferentiated Sol8 myoblast, (E) differentiating Sol8 myoblast and (F) Sol8 myotube (F+4) expressing myc- α -act G146D. Arrows indicate myc positive blebs in differentiating Sol8 myoblasts and Sol8 myotubes. Green is myc staining, red is phalloidin staining in A, D and E, troponin T staining in B, and α -actinin staining in (C) and (F). (B), (C) and (F) are confocal images. Bars, 20 μ m. (For interpretation of the references to colour in this figure legend, the reader is referred to the web version of this article.)

V370F or for mutants with no discernable biochemical defect α -act H40Y, D286G, K336I and S348L (data not shown). In undifferentiated myoblasts (data not shown) or fibroblasts this phenomenon was never observed ([16] and Fig. S1).

In addition, wider field views indicate that, in contrast to WT expressing muscle cells that are nicely differentiated, many unfused cells, transfected with mutant actin, are present at F+4 or F+5. This is shown for α -act A138P in Fig. 4A (for wider fields of muscle cells

expressing other mutants, see Fig. S2). Consistent with this is the fusion index of myotubes formed after transfection of A138P is reduced (29.4%) as compared to that of myotubes obtained after WT actin transfection (38.6%). Most of the α -act A138P expressing single cells are rounded up or spindle shaped and display blebs. A close up of such a blebbing cell expressing α -act A138P is shown in the inset in Fig. 4A'.

To approach this statistically we determined for each mutant the percentage of round or spindle shaped blebbing cells of the total transfected population after 4 days of differentiation, which is the time point where we detected most rounded cells. Inspection of the graph in Fig. 4B shows that for the majority of NM causing α -actin mutants differentiating myoblasts display indeed an increased level of this phenotype compared to WT and mock transfected cells. This is most striking for myc α -act I136M, A138P, D154N and V163L. In the latter cases, the amount of rounded cells on day F+4 is approximately 3 to 4 fold higher than for WT α -actin expressing cells. Increased rounding up, although to a lesser extent, is also observed for cells

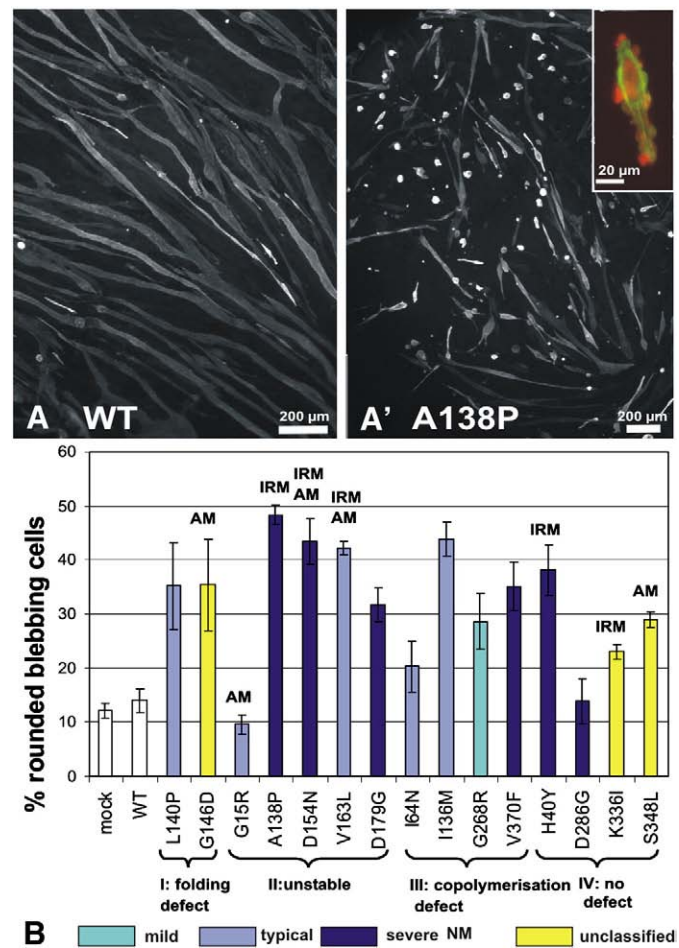


Fig. 4. The majority of α -actin mutants appear to induce cell death of muscle cells. (A, A') Wide field view of Myc-stained Sol8 cells at stage F+4. Cells expressing WT myc- α -actin are normally differentiated to myotubes (A) whereas those expressing Myc- α -act A138P (A') are poorly differentiated and many rounded up cells are observed. The inset in A' shows that myc- α -act A138P induces formation of bleb like structures in differentiating Sol8 myoblasts; Green corresponds to the myc staining and red to α -actinin staining. (B) Graph indicating the percentage of rounded blebbing α -actin mutant expressing cells in the transfected populations at stage F+4. The given percentages are the mean values of two experiments counted separately for the mutants (7 independent quantifications for WT). The total number of cells counted per experiment varies from 900 to 3000. Mutants are grouped by their biochemical defect. Classification in mild, severe and typical NM (indicated by colors) and actin myopathy (AM) and intranuclear rod myopathy (IRM) are according to Sparrow et al. [6]. (For interpretation of the references to colour in this figure legend, the reader is referred to the web version of this article.)

expressing α -act H40Y, L140P, G146D, D179G, G268R, S348L and V370F (between 2 and 3-fold more than WT expressing cells). Also for α -actin mutants I64N and K336I the amounts of rounded cells were still consistently higher than for WT α -actin expressing cells. Two mutants, α -act G15R and D286G had no significantly different levels of rounded up cells as WT α -actin. In the graph (Fig. 4B), the actin mutants are grouped per biochemical phenotype, which shows that the latter does not correlate with the degree of occurrence of the cellular phenotype. Colours indicate the type of NM the mutant induces, according to Sparrow et al. [6].

Note that in the set up we used, transfection efficiencies, measured at the myoblast stage, are approximately 60%. Consequently, this results in a mixed population of myotubes originating from transfected and untransfected myoblasts, perhaps yielding lower estimates of rounding differentiating myoblasts (compared to a culture with theoretical 100% transfection efficiencies), because of a possible dilution effect of the mutant actin when transfected cells fuse with untransfected cells. Additionally, rounded up cells tend to detach from the substrate ultimately yielding reduced numbers of differentiated fused cells (compare Fig. 4A and A') in function of time, whereas the number of cells at the start of the experiment was equal. Nevertheless our results suggest that rounding up and blebbing of cells may be a common phenotype of cells in culture expressing particular NM causing α -actin mutants and this happens regardless of a particular biochemical phenotype. To exclude effects of the myc-tag on the phenotype we expressed, in an independent experiment, untagged WT and A138P actin in a pIRES-GFP vector in parallel with myc-tagged WT actin expressing cells, and performed similar counts. Similar results were obtained for untagged and myc-tagged actin, and untagged A138P actin still induced a 4-fold increase in the occurrence of rounded blebbing cells (Fig. S3). Additionally, to rule out that the phenotype was induced by an elevated expression level of the mutant compared to the WT actin, we measured the mean fluorescence of single cells of parallel myc-stained Sol8 muscle cells at day F+4. Fig. S3 shows that myc-actin expression levels are similar in WT and A138P expressing muscle cells (Fig.S3).

3.5. NM causing α -actin mutants induce cell death with apoptotic features in differentiating muscle cells

Bleb formation and rounding up of cells are two phenotypes indicative of cell death, more particularly of apoptosis. Therefore we further investigated if apoptosis was indeed induced, using the α -actin mutant A138P as a model (for examples of other mutants see below). We did not detect increased DNA fragmentation (by TUNEL staining or isolation of genomic DNA) or phosphatidylserine externalization (by annexin V staining) (data not shown). However, we observed occasionally condensed, fragmented nuclei (Fig. 5A) as well as the release of cytochrome *c* in the cytosol which is typical for apoptosis ([23] and Fig. 5A–C). Rounded up cells expressing the A138P mutant indeed display increased diffuse cytosolic cytochrome *c* staining (Fig. 5B,C), whereas untransfected differentiating cells (Fig. 5B) or WT expressing differentiating cells show a distinct punctuate mitochondrial staining (Fig. 5D).

In striated muscle cells both a caspase- and a caspase-independent cell death pathway have been described [24,25]. We probed whether caspases were activated at early differentiation and myoblast stages using Western blot and immunohistochemistry; however, we did not observe elevated cleaved caspase species or products (caspase 3 (Fig. 5I,J, S4), 2, 6, 9 or 12, PARP data not shown). Moreover, treatment of WT and A138P expressing myotubes with the pancaspase inhibitor ZVAD-FMK, unexpectedly resulted in increased numbers of rounding cells in a dose dependent manner (Fig. 5K). The observed lack of increased caspase activity suggests that mutant expressing cells may induce the alternative caspase-independent pathway.

In this case, in skeletal muscle, apoptosis inducing factor (AIF) and endonuclease G (endo G) are released from mitochondria to the cytosol and translocate, via a stage of perinuclear localization [24] to the nucleus (reviewed in [23]). Therefore, we performed stainings for endo G and AIF on the transfected dying cells. We observed indeed perinuclear and nuclear localisation of AIF and endo G in the round cells expressing A138P (Fig. 5E, G), and a cytoplasmic staining in WT expressing cells (Fig. 5F, H).

We additionally tested whether calpain was active in this process, as it was earlier described to be involved in apoptosis in serum-deprived satellite cells [26] and to be upstream from AIF [27,28]. We incubated WT and A138P expressing myotubes with the calpain inhibitor PD150606, which inhibits both m-calpain and μ -calpain, and found that this significantly decreased the number of rounding, blebbing cells in A138P expressing cells, whereas it had no effect on cell death in the WT expressing population (Fig. 5L). This indicates that cell death is occurring, but via a less classical pathway. We will therefore refer to this as cell death with apoptotic features.

3.6. Early myotubes expressing α -actin mutants can also undergo cell death with apoptotic features

As pointed out above, in case of mutant transfections, the number of fused myotubes was often reduced. This is because dying myotubes retract from plates, round up and detach rapidly. Therefore, monitoring cell death directly in cultured myotubes is more difficult. Still the blebbing phenomenon was observed at the early myotube stage. Some of the myotubes transfected with mutants α -act I64N, I136M, A138P, L140P, D154N or D286G displayed blebs at their sarcolemma (Fig. 6A–F, Movie S5). For given mutants, blebs are either small, big or consist of piles of multiple stacked small blebs. The presence of these blebs suggests that the cell death with apoptotic features, observed in differentiating myoblasts, also occurs at later stages of differentiation. Evidence for this is presented in Fig. 6, where myotubes transfected with act L140P, display diffusely distributed cytochrome *c* in the sarcoplasm of some myotubes (Fig. 6E). This is in contrast with untransfected (Fig. 6E) or WT actin expressing myotubes (Fig. 6F) where the cytochrome *c* staining is punctuate and distinct. We saw the same diffuse staining in retracting myotubes expressing act A138P (Fig. 6G). Moreover in elongated myotubes, presumably representing an early stage of cell death before retracting and rounding, we saw an accumulation of mitochondria to the perinuclear region on cytochrome *c* staining. This is an early indication of apoptosis in several other cell types [29,30] (Fig. 6H). Myotubes transfected with α -actin A138P sometimes displayed increased perinuclear endo G staining (Fig. 6J,L, Movie S6) even after rounding up (Fig. 6K), whereas in WT myotubes this does not occur (Fig. 6I). These results show that induction of cell death can occur in differentiating myoblasts as well as in myotubes in culture expressing particular α -actin mutants causing NM.

3.7. Does the degree of induction of cell death with apoptotic features correlate with rod or aggregate formation capacity of the mutants?

The data presented above show that the investigated α -actin mutants, which are associated with NM induce various cell death related phenotypes; however, the number of dying cells is different. Therefore, we analysed if this correlates (or inversely correlates) with induction of hallmark phenotypes of nemaline myopathy: rods and aggregates, in fibroblasts or in muscle cells.

α -act H40Y, V163L [16], K336I and S348L (Fig. 7A,B) induce in many fibroblasts intranuclear rods (that stain with phalloidin) but only V163L does this to a similar extent in myoblasts and in a few cases in nascent and fused myotubes (Fig. 7C–E). For the other three mutants, rod formation is more sporadic and also not always in the nucleus (Fig. 7F,G). Similarly, for α -act I64N [16], D179G and V370F

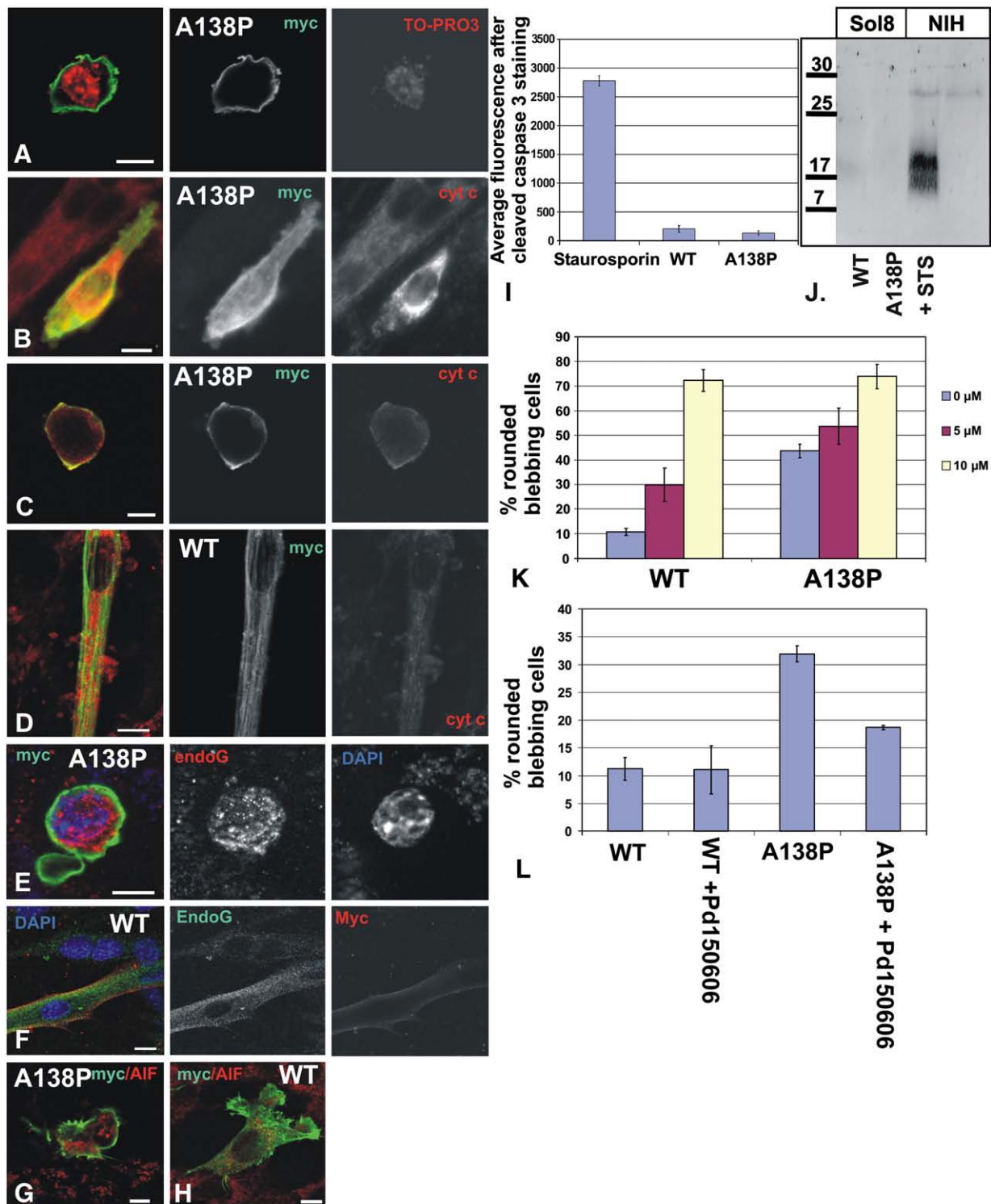
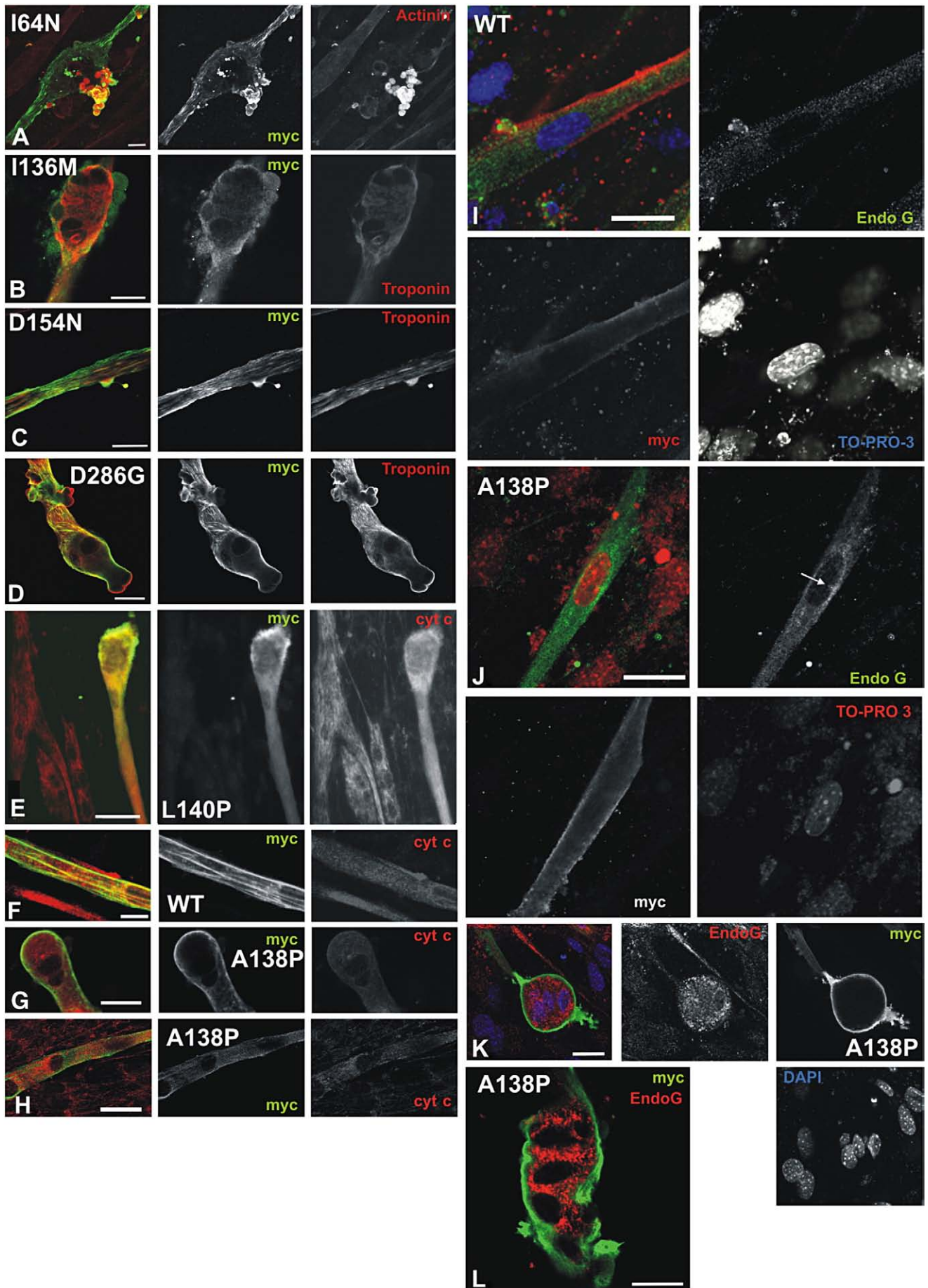


Fig. 5. The observed cell death is associated with apoptotic features in myoblasts. (A) Rounded myoblast expressing myc- α -act A138P showing a fragmented nucleus. (B) A blebbing myoblast and (C) a rounded up myoblast at day F+4 expressing myc- α -act A138P (green) show intense and/or diffuse cytoplasmic cytochrome c staining (red, compare intensities with neighbouring non-transfected cells), which is indicative of apoptosis, whereas differentiating myoblasts at day F+4 expressing WT myc- α -actin (D, green) show distinct punctuate and weaker cytochrome c staining (red). (E) Optical section (Apotome) of a round myoblast expressing myc- α -act A138P (green) with blebs and nuclear endoG localization (red); the DAPI staining showing the nucleus is in blue. (F) confocal image of differentiating myoblast expressing WT myc- α -act (red) showing punctuate endoG staining (green). (G) Differentiated myoblast expressing myc- α -act A138P or WT myc- α -act (green) with nuclear AIF localization (red) and a WT expressing cell (H). Bars, 10 μ m. (I) Average fluorescence measurement after cleaved caspase 3 immunostaining (see Fig. S2) shows no significant staining in WT and A138P myc- α -act expressing cells, compared to staurosporin incubated cells. (J) Cleaved caspase 3 blot of lysates of Sol8 expressing α -actin WT and A138P. The 17 and 19 kDa fragments of cleaved caspase 3 are seen in lysates of NIH stimulated with 1 μ M staurosporin (STS) as positive control. (K,L) Graph indicating the percentage of rounded blebbing α -actin mutant expressing cells in the transfected populations at stage F+4 of WT and A138P expressing myc- α -act upon treatment with the pancaspase inhibitor ZVAD-FMK (5 and 10 μ M) (K) or with the calpain inhibitor PD150606 (50 μ M) (L). (For interpretation of the references to colour in this figure legend, the reader is referred to the web version of this article.)



long cytoplasmic rods were frequently present in fibroblasts, but hardly in myoblasts or myotubes (Fig. S1). For myotubes expressing α -act D286G, sometimes cytoplasmic or intranuclear rods are observed (Fig. 7H,I). In general the rods in myotubes do not stain for α -actinin (Fig. 7D) or troponin T (Fig. 7E,F) but consist of F-actin as shown by phalloidin staining (Fig. 7C). However, the propensity for rod formation appears not to correlate with the degree of induction of cell death, e.g. the strong rod inducing mutant α -act V163L appears to induce a similar degree of cell death than some mutants that do not induce rods, like α -act I136M.

The mutants with compromised ATP-binding α -act D154N (this study) and G15R and V163L [16] display abundant phalloidin positive aggregates in myoblasts (e.g. G15R and D154N in Fig. 8A–B) and this parallels the observation for these mutants in fibroblasts ([16] and data not shown). Most of these mutants are to some extent also able to incorporate in actin fibers in cells consistent with their *in vitro* copolymerisation capacity (Table 1 and [16]). In differentiating myoblasts and myotubes the aggregates appear clustered as thickened fibers, which do not stain with α -actinin (Fig. 8C–F, see also [15] for G15R-GFP and V163L-GFP). In sporadic cases we managed to keep myotubes long enough in culture to obtain the striated pattern, typical for the sarcomere, as is shown in Fig. 8G for F+11 myotubes expressing WT- α -actin. In such F+11 myotubes expressing the mutants α -act D154N (Fig. 8H), V163L (Fig. 8I), and D286G (Fig. 8J) the thickened fibers become more pronounced and seem to disturb sarcomere formation. Again however there is no clear correlation between the aggregate phenotype and the degree of apoptosis induction since e.g. the mutant α -act D154N induces a substantial degree of cell death whereas for the mutant α -act G15R this is equal to WT- α -actin.

4. Discussion

4.1. NM causing α -actin mutants induce cell death with apoptotic features in cultured muscle cells

By studying a new series of NM causing α -actin mutants we unexpectedly discovered that several of these mutants induce cell death in differentiating muscle cells. This seems to happen regardless of the subtype of NM, and also regardless of the biochemical and cytoskeletal phenotype of the mutants. 13 out of 15 of the investigated mutants induce cell death in differentiating myoblasts and early myotubes. Since this phenotype was not a selection criteria for initially studying these mutants we deduce that induction of cell death in muscle cells by NM causing α -actin mutants may be a general process.

Although we did not observe hallmarks described for apoptosis, such as DNA fragmentation, phosphatidyl externalization and increased caspase activity, we could find several apoptotic related features: cells become rounded up, display blebbing and nuclear condensation. We also observed perinuclear accumulation of mitochondria, release of cytochrome *c* from mitochondria and translocation of the apoptosis markers Endo G and AIF to the nuclei or to their periphery (reviewed by [25]) [23,24]. The lack of increased caspase activity and the fact that adding a calpain inhibitor to A138P expressing cells reduced cell death suggests activation of a caspase-independent pathway in mutant expressing cells. This is consistent

with the notions that caspase-independent, but calpain-dependent pathways in muscle tissue are more important [24] and that post-mitotic apoptosis, especially in muscle, is different from apoptosis in dividing cells. The latter is in agreement with the lack of apoptosis in fibroblasts ([15,16], this study) or undifferentiated myoblasts (data not shown) upon expressing these muscle actin mutants.

The fact that inhibiting caspases increase cell death, both in WT and mutant expressing differentiating myoblasts is somewhat surprising but also argues for a caspase-independent pathway of apoptosis in the mutant expressing cells. Caspase inhibition dramatically increases the number of unfused cells, indicating a certain level of caspase activity not leading to apoptosis is required for myoblast fusion [31,32].

4.2. Why are the α -actin mutants causing cell death with apoptotic features?

An obvious explanation is a functional imbalance between WT and mutant α -actin. This may, however, occur in several ways. Mutants α -act L140P and G146D are arrested on the cellular folding machinery and may thereby interfere with folding of endogenous WT actin ultimately resulting in less functional actin. Less stable mutant monomers may partition preferentially to complexes in which they are more stable (i.e. filamentous structures in aggregates or rods) and thereby become occluded from interaction with the regular muscle actin structures, for instance during z-body formation. Mutants with copolymerization defects may affect this important process during differentiation. Therefore α -actin mutants may stimulate cell death by generating aberrant actin structures, e.g. by altered functional G/F-actin ratios. This parallels the observation that the addition of drugs, such as jasplakinolide and cytochalasin D, respectively stabilizing and destabilizing the actin cytoskeleton, results in increased apoptosis in various cell lines [33,34]. If abnormal actin structures induce cell death, it is tempting to speculate there is a sensor for cytoskeletal integrity during muscle differentiation, the nature of which remains however to be determined.

4.3. Fiber loss in NM-patient muscle might be caused by cell death of differentiating muscle cells expressing α -actin mutants

Our data open a scenario in which patients may have increased proportions of dying muscle cells. Demonstrating the occurrence of cell death in muscle tissue of patients is, however, difficult, since dying (apoptotic) cells are rapidly eliminated by phagocytosis by resident cells to avoid inflammatory reactions [35,36]. This is likely the reason why increased cell death, or apoptosis has not yet been uncovered in NM muscle biopsies. Yet, it has been shown that apoptotic mechanisms occur in various other myopathies and in muscle fiber atrophy in patients [35–37] or in rodent models. It also has been shown that calpains are involved in different types of muscle atrophy, such as Duchenne muscular dystrophy, limb-girdle muscular dystrophy and sarcopenia (reviewed in [38]).

Of relevance is that in rat models of age-related atrophy the EndoG and AIF content is increased [39,40] suggesting caspase-independent cell death contributes to preferential loss of type II muscle fibers during sarcopenia [24,41]. This is consistent with both the commonly

Fig. 6. Apoptosis also occurs at the myotube stage. Examples of various apoptosis related phenotypes for several mutants are presented. (A) Primary myotube displaying blebs upon expression of myc- α -act I64N; (B) sol8 myotube displaying blebs upon expression of myc- α -act I136M; (C) primary myotube expressing myc- α -act D154N, in addition to small blebs, pinched of “vesicle-like structures” were observed; (D) a twisted primary myotube expressing myc- α -act D286G displays big blebs. Green: myc staining, red: α -actinin staining in A, troponin T staining in (B–D); images are confocal. (E) Myotube expressing myc- α -act L140P (green) undergoing apoptosis as deduced from membrane blebbing and diffuse cytochrome *c* staining (red) whereas myotubes expressing WT myc- α -actin (F, green) show distinct punctuate cytochrome *c* staining (red). (G, H) Confocal image of a retracting myotube (G) or elongated myotube (H) expressing myc- α -act A138P (green) with diffuse staining (G) perinuclear accumulation (H) of cytochrome *c* staining (red). (I) Confocal images of myotubes transfected with WT myc- α -actin, with regular punctate endo G staining (red); the nucleus is in blue. (J) Confocal image of myotube transfected with myc- α -act A138P (green), with nuclear (arrow) and perinuclear enriched endo G staining (red). (K) Optical section showing rounded up cells transfected with myc- α -act A138P (green), containing multiple nuclei where endo G (red) is partly translocated to these nuclei (blue). (L) Retracting myotube transfected with myc- α -act A138P (green), with nuclear and perinuclear enriched endo G staining (red). Bars, 20 μ m. (For interpretation of the references to colour in this figure legend, the reader is referred to the web version of this article.)

observed atrophy in NM patients, with a lack of type II fibers [6] and our observation that expression of α -actin mutants induces AIF and Endo G mediated cell death in cell cultures. Additionally, biopsies of a

NM-patient with mutation G268D showed that muscle tissue was progressively replaced by connective and fat tissue [42], which may be explained by cell death. Such fibrosis and adiposis is also a common feature in the dystrophies mentioned above that are associated with calpain-dependent cell death [43,44]. Moreover induction of cell death by mutations leading to NM may not be restricted to α -actin. An NM mouse model carrying the tropomyosin-3 mutation M9R showed upregulation of cell death proteins in two types of muscle, next to degeneration of fibers, abnormal mitochondria and delayed muscle maturation [45]. This also raises the possibility that the loss of muscle tissue triggers regeneration through the activation of satellite cells to terminal differentiation. In these stimulated cells the expression of the mutant actin could lead to calpain-dependent cell death and thus to less efficient muscle repair.

4.4. Cell death versus other NM associated phenotypes

Our data suggest that cell death is a common phenotype of differentiating muscle cells expressing NM causing α -actin mutants. Yet this may not be the only defect in NM. Indeed for two mutants, α -act G15R and D286D, we found no evidence for post-mitotic cell death. We cannot exclude cell death occurring at later stages of differentiation but the fact that these mutants produce thickened fibers suggests that disturbed muscle ultrastructure may also cause NM. Indeed, some myotubes expressing cell death inducing mutants (α -act D154N, V163L), escape the process and display abnormal actin-based structures such as thickened fibers. This leaves open the possibility that both phenotypes lead to muscle weakness albeit via different routes. Other examples where cell death likely does not contribute to NM are the recessive lethal mutations. The mutant proteins are folding defective [16] and newborns die because they have no functional striated muscle α -actin.

For the mutants we tested, we found no correlation between the severity of the disease and the number of dying cells in cell cultures. This is consistent with the fact that the presence of muscle fiber atrophy was also not correlated with the clinical presentation of NM patients in a large-scale study [1]. One might however expect that increased cell death is most important in severe NM, where cell death reduces the muscle mass dramatically, resulting in mortality short after birth. As is shown in a mouse model with a α -tropomyosin mutation, in milder forms of NM, muscle function might increase through exercise [46], suggesting cell death might be less prominent here. However, we think cell death is a common phenotype partly responsible for the observed atrophy and may, perhaps indirectly, be responsible for muscle weakness in NM patients.

Our discovery of calpain-dependent cell death as a new and fairly common phenotype induced by α -actin mutants, support the more current view that rods and aggregates are not the major cause of NM pathogenesis [45,46]. Indeed, for most of the mutants we observed that rod formation is less frequent in differentiating muscle cells than in fibroblasts, which were initially used to characterize NM causing α -actin mutants ([16] and this study). In addition, it has been reported that hypotonia manifests itself in NM patients before rods become visible in biopsies [1,47] and that the proportion of

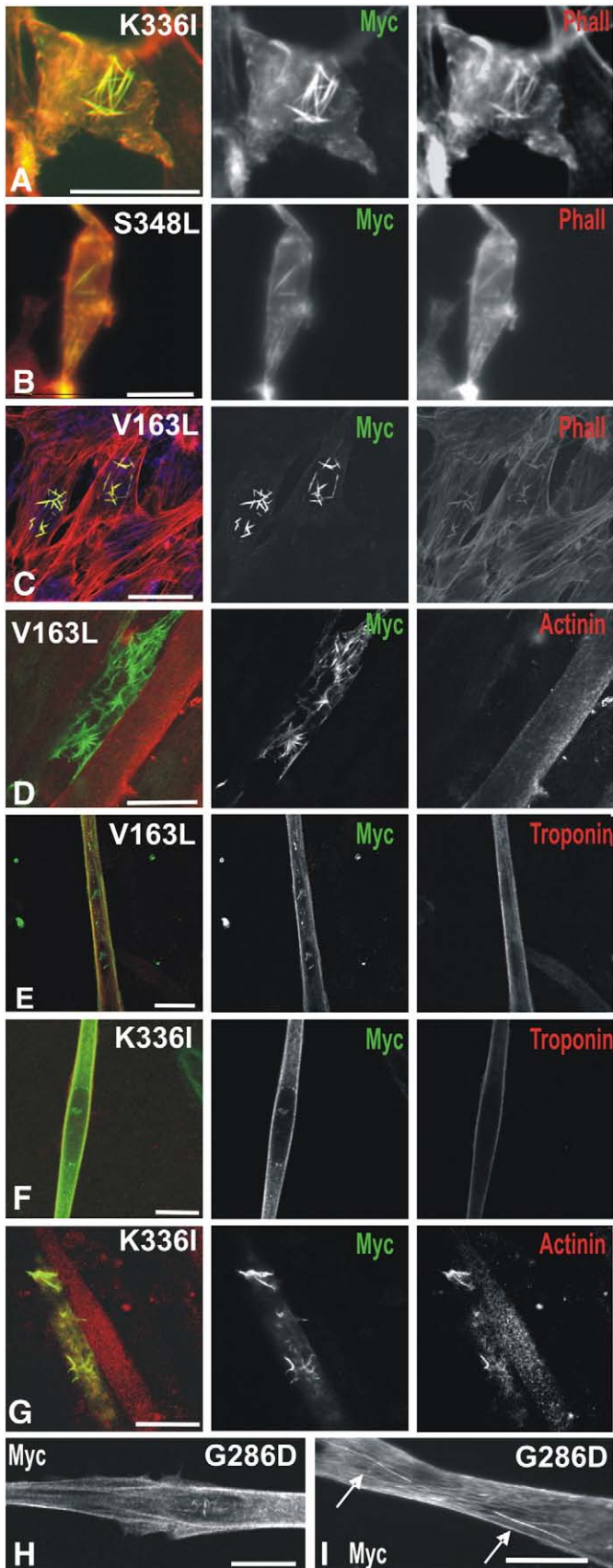


Fig. 7. Several α -actin mutants induce actin rod formation in cell culture. Myc- α -act K336I (A) and myc- α -act S348L (B) induce intranuclear rod formation in NIH3T3 fibroblasts. (C-E) Examples of rod formation induced by expression of myc- α -act V163L in (C) undifferentiated Sol8 myoblasts (intranuclear rods); in (D) a nascent myotube full of rods, in (E) a primary myotube (intranuclear rods); (F,G) primary myotube expressing myc- α -act K336I display sometimes intranuclear rod formation (F) or cytoplasmic rod formation (G). (H,I) Myotubes expressing myc- α -act G286D display intranuclear (H) or cytoplasmic (I) rod formation. Green in (A-G) corresponds to myc staining, red to phalloidin staining in (A-C), to α -actinin staining in (D) and (G) or troponin T staining in (E) and (F) and blue to TO-PRO-3 staining in (C). (H) and (I) are myc staining. Bars, 20 μ m. (For interpretation of the references to colour in this figure legend, the reader is referred to the web version of this article.)

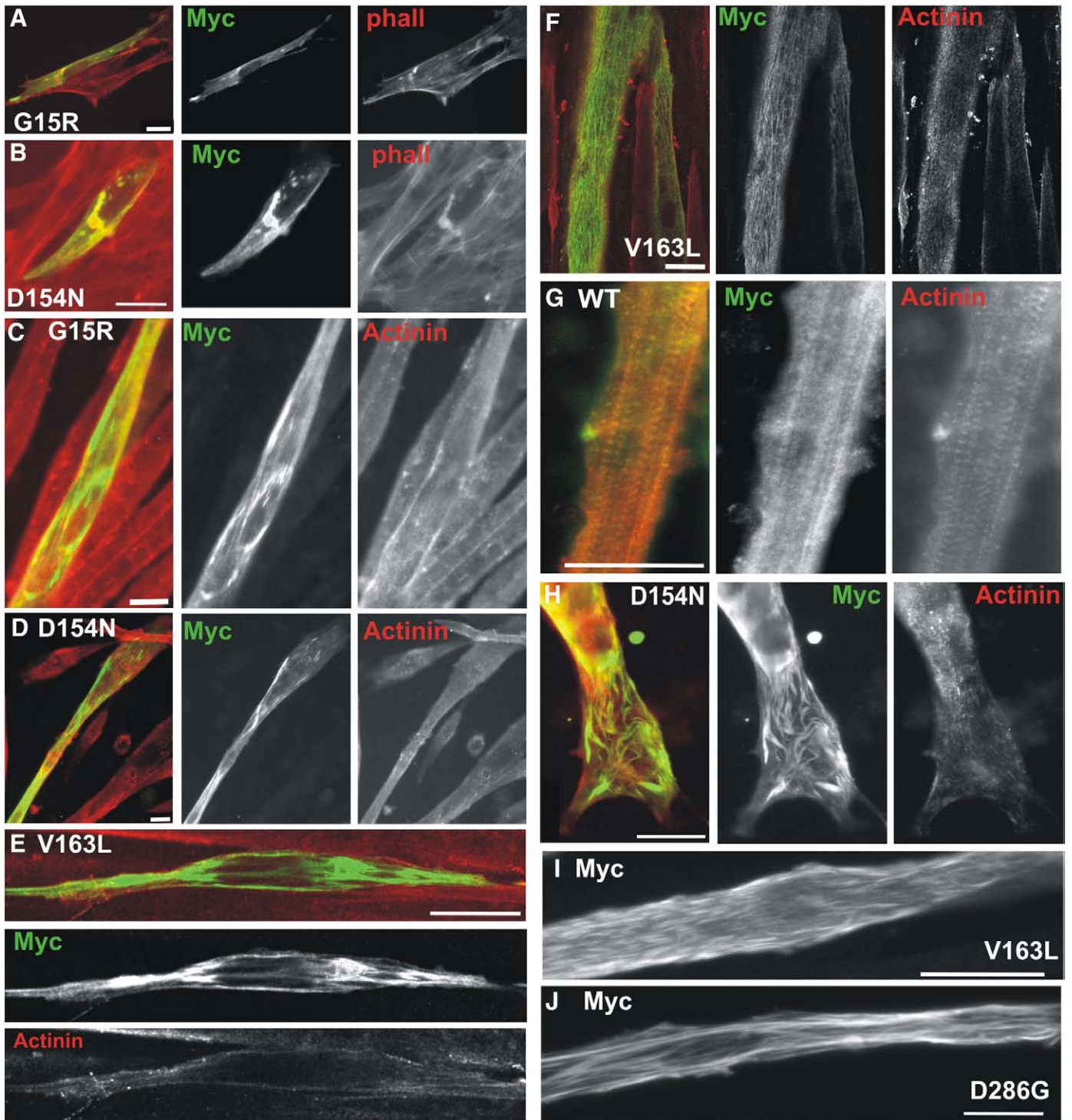


Fig. 8. Actin mutants with compromised ATP-binding cause aggregate formation. (A, B) Sol8 myoblasts expressing myc- α -act G15R (A) or myc- α -act D154N (green) (B) have phalloidin (red) positive aggregates. Sol8 myotubes (F+4) expressing myc- α -act G15R (C) or myc- α -act D154N (D) have thickened fibers containing the mutant as do Sol8 myotube (F+4) expressing myc- α -act V163L (E). (G) Sol8 myotube (F+11) expressing WT- α -actin displays the regular striation pattern whereas in Sol8 myotube (F+11) expressing myc- α -act D154N (H), Sol8 myotube (F+11) expressing myc- α -act V163L (I) and Sol8 myotube (F+11) expressing myc- α -act D286G (J) is disturbed and thickened fibers are present. Green in (C–H) corresponds to myc staining and red to α -actinin staining, myc staining in (I) and (J). Bars, 20 μ m. (For interpretation of the references to colour in this figure legend, the reader is referred to the web version of this article.)

fibers containing rods does not correlate with the degree of muscle weakness [2]. Therefore actin rod formation (and aggregate formation), may be a secondary effect and perhaps a way for the cell to get rid of defective actins, as rods are also found in brains of dystonia patients carrying the β -actin mutation R183W [48]. The assumption that actin rods and aggregates may be secondary effects does not

mean they are harmless, since patient biopsies show that rods or aggregates severely disturb muscle ultrastructure (see e.g. [49] Fig. 3 and [42] Fig. 1 for rods, and [50] for aggregates caused by α -act D154N). This suggests that cytoplasmic rods and aggregates may also contribute to malfunction of muscles at later stages of the disease.

4.5. Conclusion

In the present study, a picture emerges that calpain involved muscle cell death may be a major, common and primary defect induced by NM causing dominant negative α -skeletal muscle actin mutants. In this scenario, this should lead to muscle fiber loss which is consistent with observed atrophy in patients. However, we consider it unlikely that this is the sole cause of this heterogeneous disease, since cell death is usually not the only phenotype observed in cell cultures and, depending on the particular mutant a significant proportion of cells escape cell death. Those that do, display major ultrastructure disorganisation. Therefore both phenomena can contribute to muscle weakness.

Acknowledgements

We thank Prof. J. Gettemans for use of the Zeiss apotome. This work was supported by grants FWO-G0133.06 (to C.A. and H.R.), GOA-12051401, to J.V. and C.A., IWT-51185 to D.V. and grants from the CNRS, the French Ministry for scientific research, French Association against Myopathies to BC.

Appendix A. Supplementary data

Supplementary data associated with this article can be found, in the online version, at doi:10.1016/j.bbamcr.2009.04.004.

References

- M.M. Ryan, B. Ilkovski, C.D. Strickland, C. Schnell, D. Sanoudou, C. Midgett, R. Houston, D. Muirhead, X. Dennett, L.K. Shield, U. De Girolami, S.T. Iannaccone, N.G. Laing, K.N. North, A.H. Beggs, Clinical course correlates poorly with muscle pathology in nemaline myopathy, *Neurology* 60 (2003) 665–673.
- D. Sanoudou, A.H. Beggs, Clinical and genetic heterogeneity in nemaline myopathy—a disease of skeletal muscle thin filaments, *Trends Mol. Med.* 7 (2001) 362–368.
- E. Clarkson, C.F. Costa, L.M. Machesky, Congenital myopathies: diseases of the actin cytoskeleton, *J. Pathol.* 204 (2004) 407–417.
- B. Ilkovski, S.T. Cooper, K. Nowak, M.M. Ryan, N. Yang, C. Schnell, H.J. Durling, L.G. Roddick, I. Wilkinson, A.J. Kornberg, K.J. Collins, G. Wallace, P. Gunning, E.C. Hardeman, N.G. Laing, K.N. North, Nemaline myopathy caused by mutations in the muscle alpha-skeletal-actin gene, *Am. J. Hum. Genet.* 68 (2001) 1333–1343.
- K.J. Nowak, D. Wattanasirichaigoon, H.H. Goebel, M. Wilce, K. Pelin, K. Donner, R.L. Jacob, C. Hubner, K. Oexle, J.R. Anderson, C.M. Verity, K.N. North, S.T. Iannaccone, C.R. Muller, P. Nurnberg, F. Muntioni, C. Sewry, I. Hughes, R. Sutphen, A.G. Lacson, K.J. Swoboda, J. Vigneron, C. Wallgren-Pettersson, A.H. Beggs, N.G. Laing, Mutations in the skeletal muscle alpha-actin gene in patients with actin myopathy and nemaline myopathy, *Nat. Genet.* 23 (1999) 208–212.
- J.C. Sparrow, K.J. Nowak, H.J. Durling, A.H. Beggs, C. Wallgren-Pettersson, N. Romero, I. Nonaka, N.G. Laing, Muscle disease caused by mutations in the skeletal muscle alpha-actin gene (*ACTA1*), *Neuromuscul. Disord.* 13 (2003) 519–531.
- M. Yamaguchi, R.M. Robson, M.H. Stromer, D.S. Dahl, T. Oda, Nemaline myopathy rod bodies. Structure and composition, *J. Neurol. Sci.* 56 (1982) 35–56.
- J. Gurgel-Giannetti, U. Reed, M.L. Bang, K. Pelin, K. Donner, S.K. Marie, M. Carvalho, M.A. Fireman, E. Zanoteli, A.S. Oliveira, M. Zatz, C. Wallgren-Pettersson, S. Labeit, M. Vainzof, Nebulin expression in patients with nemaline myopathy, *Neuromuscul. Disord.* 11 (2001) 154–162.
- K.J. Nowak, C.A. Sewry, C. Navarro, W. Squier, C. Reina, J.R. Ricoy, S.S. Jayawant, A.M. Childs, J.A. Dobbie, R.E. Appleton, R.C. Mountford, K.R. Walker, S. Clement, A. Barois, F. Muntioni, N.B. Romero, N.G. Laing, Nemaline myopathy caused by absence of alpha-skeletal muscle actin, *Ann. Neurol.* 61 (2007) 175–184.
- C. Wallgren-Pettersson, N.G. Laing, 138th ENMC Workshop: nemaline myopathy, 20–22 May 2005, Naarden, the Netherlands, *Neuromuscul. Disord.* 16 (2006) 54–60.
- Y. Gao, J.O. Thomas, R.L. Chow, G.H. Lee, N.J. Cowan, A cytoplasmic chaperonin that catalyzes beta-actin folding, *Cell* 69 (1992) 1043–1050.
- K. Neiryck, D. Waterschoot, J. Vandekerckhove, C. Ampe, H. Rommelaere, Actin interacts with CCT via discrete binding sites: a binding transition-release model for CCT-mediated actin folding, *J. Mol. Biol.* 355 (2006) 124–138.
- I.E. Vainberg, S.A. Lewis, H. Rommelaere, C. Ampe, J. Vandekerckhove, H.L. Klein, N.J. Cowan, Prefoldin, a chaperone that delivers unfolded proteins to cytosolic chaperonin, *Cell* 93 (1998) 863–873.
- J.E. Estes, L.A. Selden, H.J. Kinoshita, L.C. Gershman, Tightly-bound divalent cation of actin, *J. Muscle Res. Cell Motil* 13 (1992) 272–284.
- F.S. Bathe, H. Rommelaere, L.M. Machesky, Phenotypes of myopathy-related actin mutants in differentiated C2C12 myotubes, *BMC Cell Biol.* 8 (2007) 2.
- C.F. Costa, H. Rommelaere, D. Waterschoot, K.K. Sethi, K.J. Nowak, N.G. Laing, C. Ampe, L.M. Machesky, Myopathy mutations in alpha-skeletal-muscle actin cause a range of molecular defects, *J. Cell. Sci.* 117 (2004) 3367–3377.
- B. Ilkovski, K.J. Nowak, A. Domazetovska, A.L. Maxwell, S. Clement, K.E. Davies, N.G. Laing, K.N. North, S.T. Cooper, Evidence for a dominant-negative effect in ACTA1 nemaline myopathy caused by abnormal folding, aggregation and altered polymerization of mutant actin isoforms, *Hum. Mol. Genet.* 13 (2004) 1727–1743.
- H. Rommelaere, D. Waterschoot, K. Neiryck, J. Vandekerckhove, C. Ampe, A method for rapidly screening functionality of actin mutants and tagged actins, *Biol. Proced. Online* 6 (2004) 235–249.
- C. Mulle, P. Benoit, C. Pinset, M. Roa, J.P. Changeux, Calcitonin gene-related peptide enhances the rate of desensitization of the nicotinic acetylcholine receptor in cultured mouse muscle cells, *Proc. Natl. Acad. Sci. U. S. A.* 85 (1988) 5728–5732.
- H. Rommelaere, D. Waterschoot, K. Neiryck, J. Vandekerckhove, C. Ampe, Structural plasticity of functional actin: pictures of actin binding protein and polymer interfaces, *Structure (Camb)* 11 (2003) 1279–1289.
- W. Kabsch, J. Vandekerckhove, Structure and function of actin, *Annu. Rev. Biophys. Biomol. Struct.* 21 (1992) 49–76.
- P. Gunning, V. Ferguson, K. Brennan, E. Hardeman, Impact of alpha-skeletal actin but not alpha-cardiac actin on myoblast morphology, *Cell. Struct. Funct.* 22 (1997) 173–179.
- M. van Gurp, N. Festjens, G. van Loo, X. Saelens, P. Vandenabeele, Mitochondrial intermembrane proteins in cell death, *Biochem. Biophys. Res. Commun.* 304 (2003) 487–497.
- E.E. Dupont-Versteegden, Apoptosis in skeletal muscle and its relevance to atrophy, *World J. Gastroenterol.* 12 (2006) 7463–7466.
- E. Marzetti, C. Leeuwenburgh, Skeletal muscle apoptosis, sarcopenia and frailty at old age, *Exp. Gerontol.* 41 (2006) 1234–1238.
- L.J. Mampuru, S.J. Chen, J.L. Kalenik, M.E. Bradley, T.C. Lee, Analysis of events associated with serum deprivation-induced apoptosis in C3H/Sol8 muscle satellite cells, *Exp. Cell Res.* 226 (1996) 372–380.
- C. Artus, E. Maquarre, R.S. Moubarak, C. Delettre, C. Jasmin, S.A. Susin, J. Robert-Lezennes, CD44 ligation induces caspase-independent cell death via a novel calpain/AIF pathway in human erythroleukemia cells, *Oncogene* 25 (2006) 5741–5751.
- E. Norberg, V. Gogvadze, M. Ott, M. Horn, P. Uhlen, S. Orrenius, B. Zhivotovskiy, An increase in intracellular Ca(2+) is required for the activation of mitochondrial calpain to release AIF during cell death, *Cell Death Differ.* 15 (2008) 1857–1864.
- N.G. Calvo, C.R. Gentili, A.R. de Boland, The early phase of programmed cell death in Caco-2 intestinal cells exposed to PTH, *J. Cell. Biochem.* 105 (2008) 989–999.
- B. Pucci, F. Bertani, N.O. Karpnich, M. Indelicato, M.A. Russo, J.L. Farber, M. Tafani, Detailing the role of Bax translocation, cytochrome c release, and perinuclear clustering of the mitochondria in the killing of HeLa cells by TNF, *J. Cell. Physiol.* 217 (2008) 442–449.
- T.V. Murray, J.M. McMahon, B.A. Howley, A. Stanley, T. Ritter, A. Mohr, R. Zwacka, H.O. Fearnhead, A non-apoptotic role for caspase-9 in muscle differentiation, *J. Cell. Sci.* 121 (2008) 3786–3793.
- P. Fernando, J.F. Kelly, K. Balazsi, R.S. Slack, L.A. Megeney, Caspase 3 activity is required for skeletal muscle differentiation, *Proc. Natl. Acad. Sci. U. S. A.* 99 (2002) 11025–11030.
- S.C. Posey, B.E. Bierer, Actin stabilization by jasplakinolide enhances apoptosis induced by cytokine deprivation, *J. Biol. Chem.* 274 (1999) 4259–4265.
- Y. Yamazaki, M. Tsuruga, D. Zhou, Y. Fujita, X. Shang, Y. Dang, K. Kawasaki, S. Oka, Cytoskeletal disruption accelerates caspase-3 activation and alters the intracellular membrane reorganization in DNA damage-induced apoptosis, *Exp. Cell Res.* 259 (2000) 64–78.
- M. Sandri, U. Carraro, Apoptosis of skeletal muscles during development and disease, *Int. J. Biochem. Cell Biol.* 31 (1999) 1373–1390.
- D.S. Tews, Apoptosis and muscle fibre loss in neuromuscular disorders, *Neuromuscul. Disord.* 12 (2002) 613–622.
- D.S. Tews, W. Behrhof, S. Schindler, SMAC-expression in denervated human skeletal muscle as a potential inhibitor of coexpressed inhibitor-of-apoptosis proteins, *Appl. Immunohistochem. Mol. Morphol.* 16 (2008) 66–70.
- E. Dargelos, S. Poussard, C. Brule, L. Daury, P. Cottin, Calcium-dependent proteolytic system and muscle dysfunctions: a possible role of calpains in sarcopenia, *Biochimie* 90 (2008) 359–368.
- C. Leeuwenburgh, C.M. Gurley, B.A. Strotman, E.E. Dupont-Versteegden, Age-related differences in apoptosis with disuse atrophy in soleus muscle, *Am. J. Physiol., Regul. Integr. Comp. Physiol.* 288 (2005) R1288–1296.
- P.M. Siu, E.E. Pistilli, S.E. Alway, Apoptotic responses to hindlimb suspension in gastrocnemius muscles from young adult and aged rats, *Am. J. Physiol., Regul. Integr. Comp. Physiol.* 289 (2005) R1015–1026.
- L. Larsson, B. Sjodin, J. Karlsson, Histochemical and biochemical changes in human skeletal muscle with age in sedentary males, age 22–65 years, *Acta Physiol. Scand.* 103 (1978) 31–39.
- M. Ohlsson, H. Tajsharghi, N. Darin, M. Kyllerman, A. Oldfors, Follow-up of nemaline myopathy in two patients with novel mutations in the skeletal muscle alpha-actin gene (*ACTA1*), *Neuromuscul. Disord.* 14 (2004) 471–475.
- A. Emery, *Duchenne Muscular Dystrophy*, Oxford University press, Oxford, UK, 1993.
- C.D. Reimers, B. Schlotter, B.M. Eicke, T.N. Witt, Calf enlargement in neuromuscular diseases: a quantitative ultrasound study in 350 patients and review of the literature, *J. Neurol. Sci.* 143 (1996) 46–56.
- D. Sanoudou, M.A. Corbett, M. Han, M. Ghoddusi, M.A. Nguyen, N. Vlahovich, E.C. Hardeman, A.H. Beggs, Skeletal muscle repair in a mouse model of nemaline myopathy, *Hum. Mol. Genet.* 15 (2006) 2603–2612.
- J.E. Joya, A.J. Kee, V. Nair-Shalliker, M. Ghoddusi, M.A. Nguyen, P. Luther, E.C. Hardeman, Muscle weakness in a mouse model of nemaline myopathy can be reversed with exercise and reveals a novel myofiber repair mechanism, *Hum. Mol. Genet.* 13 (2004) 2633–2645.

- [47] H. Goez, L.B. Sira, J. Jossiphov, Z. Borochowitz, H. Durling, N.G. Laing, Y. Nevo, Predominantly upper limb weakness, enlarged cisterna magna, and borderline intelligence in a child with de novo mutation of the skeletal muscle alpha-actin gene, *J. Child Neurol.* 20 (2005) 236–239.
- [48] V. Procaccio, G. Salazar, S. Ono, M.L. Styers, M. Gearing, A. Davila, R. Jimenez, J. Juncos, C.A. Gutekunst, G. Meroni, B. Fontanella, E. Sontag, J.M. Sontag, V. Faundez, B.H. Wainer, A mutation of beta-actin that alters depolymerization dynamics is associated with autosomal dominant developmental malformations, deafness, and dystonia, *Am. J. Hum. Genet.* 78 (2006) 947–960.
- [49] C. Schnell, A. Kan, K.N. North, 'An artefact gone awry': identification of the first case of nemaline myopathy by Dr. R.D.K. Reye, *Neuromuscul. Disord.* 10 (2000) 307–312.
- [50] J.M. Schroder, H. Durling, N. Laing, Actin myopathy with nemaline bodies, intranuclear rods, and a heterozygous mutation in ACTA1 (Asp154Asn), *Acta Neuropathol. (Berl)* 108 (2004) 250–256.
- [51] P.B. Agrawal, C.D. Strickland, C. Midgett, A. Morales, D.E. Newburger, M.A. Poulos, K.K. Tomczak, M.M. Ryan, S.T. Iannaccone, T.O. Crawford, N.G. Laing, A.H. Beggs, Heterogeneity of nemaline myopathy cases with skeletal muscle alpha-actin gene mutations, *Ann. Neurol.* 56 (2004) 86–96.
- [52] E.A. McCormack, O. Llorca, J.L. Carrascosa, J.M. Valpuesta, K.R. Willison, Point mutations in a hinge linking the small and large domains of beta-actin result in trapped folding intermediates bound to cytosolic chaperonin CCT, *J. Struct. Biol.* 135 (2001) 198–204.